Shot noise and conductance in metallic carbon nanotubes in the presence of correlated defects

Qiang Zhang,[1] Huatong Yang,[1] Chao Zhang,[2] and Zhongshui Ma[1,2]
[1]*School of Physics, Peking University, Beijing 100871, China*
[2]*School of Engineering Physics, University of Wollongong, New South Wales 2522, Australia*
(Received 12 January 2006; revised manuscript received 14 April 2006; published 30 June 2006)

We investigate the effect of isolated scattering centers on the electronic transport in metallic carbon nanotubes. It is found that the impurity potential significantly alters the overlap of electronic wave functions and results in a rapid oscillation in the conductance and the shot noise. Furthermore, the conductance and the shot noise near the neutral Fermi energy depend periodically on the relative position of the scatterers and on the phase factor ϕ which is generated by the scattering. If two defects are in the same sublattice and $\Delta\mathbf{d} \gg a_c$, the conductance near the neutral Fermi energy is dropped to $G_0=2e^2/h$ approximately and the shot noise decreases to zero when $\phi=1$, but the conductance decreases to zero if $\phi=\omega$ or ω^2; whereas, the situation is reversed for the configuration in which two defects are in the different sublattices. For the case of closely paired defects, it is predicated that a small "energy gap" would be developed in "metallic" nanotubes. A comparison of our numerical results and the analytical calculations of the effective-mass approximation is presented.

DOI: 10.1103/PhysRevB.73.235438 PACS number(s): 73.63.Fg, 72.10.Fk, 72.70.+m

I. INTRODUCTION

Carbon nanotubes (CNTs) have attracted much attention in the last decade because of their special electrical properties and potential applications in nanodevices.[1–8] Theoretical and experimental investigations have revealed that the electronic structures of CNTs depend only on their geometries and are characterized by chirality vectors (n,m).[9] It is found that CNTs are metallic if the differences $n-m$ are multiples of 3, otherwise, they are semiconducting. The exact metallic phase of the single-walled nanotube (SWNT) may be modified by various interactions such as the intertube interaction. As an example, it has been shown that the finite tube curvature alters the overlap of the π-electron wave function and may result in a small energy gap in a metallic tube.[10]

The key to the development of CNTs-based electronic devices is the method in controlling and tuning their electronic properties. Recent progress in experimental techniques has made it possible to fabricate a CNTs-based system with controllable defects or damages. Experimental observation shows that the atoms in a CNT can be released under electron or ion irradiations effectively, and some vacancies are left in SWNTs behind.[11] A single vacancy can reduce the conductance at neutral Fermi energy to one-half of that of a perfect tube.[12,13] Therefore, artificially introducing defects represent a promising method of realizing this goal is to create some local scattering centers if it is controllable and reversible. By using the voltage pulses from a metal-coated antiferromagnetic tip[14] or the high-energy electron beam[15] to cause the local damages in CNTs, local defects can be created. Recently, Yuzvinsky *et al.*[16] reported a method of removing material locally from carbon nanotubes with the low-energy focused electron beam of a scanning electron microscope. Because clean precise cuts can be made onto nanotubes, the electronic transport properties of the CNTs devices are, then, modified.

Many important information on the electron transport can be obtained from the conductance characteristics. Like the conductance, the shot noise can be used to characterize the transport properties of mesoscopic conductors.[17–21] It stems from the charge quantization and is fundamentally connected to the statistical properties of the entities which generate the noise.[22] The shot noise is rather remarkable in experiments for mesoscopic systems. In a quantum microstructure, the fluctuations arise from the quantum-probabilistic character of electrons transmitted through the sample. The shot noise is suppressed in systems where electron transport is perfectly ballistic. Only for ideal perfect CNTs free of any disorders and external disturbance, one would not observe any detectable shot noise. However, it is inevitable in CNTs due to various disturbances such as the impurities, external fields, or distortions under pressure. The shot noise has been measured in CNTs bundles [23] and in SWNTs.[24] In the present paper we investigate theoretically and numerically the electron transport and shot noise in CNTs with paired defects whose positions are correlated. The defects are regarded as local scattering centers here. The interference between wave functions scattered from these local defects would lead to oscillations in both the conductance and the shot noise. We will investigate how the conductance and the shot noise depend on the geometrical configurations of paired defects on the CNTs and study the effect of correlated defects in the electronic transport. The studies shows that a "gap" would be generated at the neutral Fermi energy and a dip in conductance is emerged when the distance of two defects $\Delta\mathbf{d}$ is small. Unanimously, the shot noise is an oscillatory function of the relative distance when $\Delta\mathbf{d}$ is much greater than C-C bonds length. In Sec. II, the model and the calculation method will briefly be described. Section III presents the numerical results of the conductance and the shot noise is presented in the Sec. III. Using the effective mass theory,[25] thecharacteristic behaviors near the neutral Fermi energy are investigated analytically. The conclusions are summarized in Sec. IV.

II. MODEL AND METHOD

We consider an armchair CNT with two defects on it. The structure of a two-dimensional (2D) graphite (a) and corre-

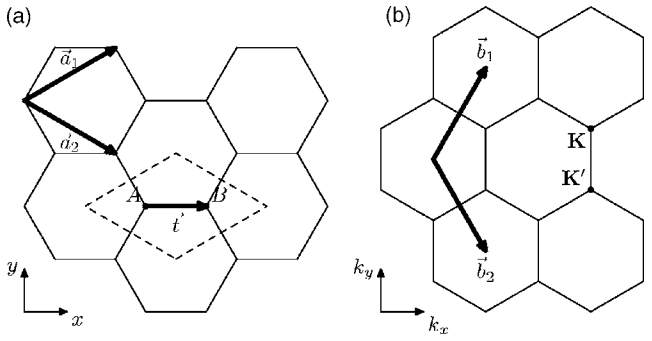

FIG. 1. (a) Graphite lattice. The y axes are along the armchair axes. The unit lattice vectors are $\vec{a}_1$ and $\vec{a}_2$. $\vec{t}$ is the vector connecting two neighboring atoms. (b) $\vec{b}_1$ and $\vec{b}_2$ are the reciprocal lattice vectors.

sponding Brillouin zone (b) are shown in Fig. 1. For simplicity, two defects are the same and are located on two different carbon atomic sites in CNT. Since the position of the first defect can be chosen to be the origin, then the second defect is located at $\Delta\mathbf{d}$,

$$\Delta\mathbf{d} = l_1\mathbf{a}_1 + l_2\mathbf{a}_2 + \lambda\mathbf{t}, \tag{1}$$

where $\mathbf{a}_1$ and $\mathbf{a}_2$ are the unit lattice vectors of the 2D graphite, while l_1 and l_2 are integers, and $\mathbf{t}=(\frac{1}{3})(\mathbf{a}_1+\mathbf{a}_2)$ is the vector which connects two neighboring atoms A and B (as seen in Fig. 1). It is easy to see that two defects are located on the same sublattice if $\lambda=0$, while two defects are located on different sublattices if $\lambda=1$. In our approach, the scattering potentials due to the defects are modeled by two pointlike potentials. It is assumed that two defects are located at $\mathbf{r_1}$ and $\mathbf{r_2}$, respectively. From Eq. (1) we have $\mathbf{r_2}-\mathbf{r_1}=\Delta\mathbf{d}$. The defects are described by a short-range potential, $V(\mathbf{r})=g[\delta(\mathbf{r}-\mathbf{r_1})+\delta(\mathbf{r}-\mathbf{r_2})]$ with the strength g.

The conductance at zero temperature can be calculated by the Landauer-Büttiker formula $G=(2e^2/h)\mathrm{Tr}\,T$. The transmission coefficient is given by $T=[\Gamma_L G^r \Gamma_R G^a]$ (Ref. 26) with $\Gamma_{L(R)}=i[\Sigma^r_{L(R)}-\Sigma^a_{L(R)}]$, where $\Sigma^r_{L(R)}=(\Sigma^a_{L(R)})^\dagger$ is the self-energy due to the left (right) lead, and $G^{r(a)}$ is the retarded (advanced) Green function of SWNT. It is found to be

$$G^r = (\epsilon^+ - H_C - \Sigma^r_L - \Sigma^r_R)^{-1} \tag{2}$$

and $G^a=(G^r)^\dagger$, where $\epsilon^+=\epsilon+i0^+$ and H_C is the Hamiltonian of the center part of nanotube. The effects of leads are completely incorporated into the self-energy $\Sigma^r_{L(R)}$. Considering the leads to be semi-infinite, the self-energy $\Sigma^r_{L(R)}$ can be written as

$$\Sigma^r_L = h^\dagger_{LC} g^r_L h_{LC}, \quad \Sigma^r_R = h_{CR} g^r_R h^\dagger_{CR}, \tag{3}$$

where h_{LC} (h_{RC}) is the coupling matrix which is determined by the geometry of connection between the conductor and the left (right) surface of contact. $g^r_{L(R)}$ are the Green's functions of the left (right) lead. Regarding the semi-infinite leads as the infinite stacks of elementary layers with nearest-neighbor interactions, the original system can be transformed into a linear chain of elementary layers. Then, we can use the method given in Refs. 27 and 28 to define T_h and $\bar{T}_h$. The Green functions are given by $G_{10}=T_h G_{00}$ and $G_{01}=G_{00}\bar{T}_h$. The self-energies are found to be $\Sigma^r_R=h_{01}T_h$ and $\Sigma^r_L=\bar{T}_h h^\dagger_{01}$. According to Refs. 27 and 28, T_h and $\bar{T}_h$ can be computed with the formulas

$$T_h = t_0 + \tilde{t}_0 t_1 + \tilde{t}_0\tilde{t}_1 t_2 + \cdots + \tilde{t}_0\tilde{t}_1\tilde{t}_2\cdots t_n$$

and

$$\bar{T}_h = \tilde{t}_0 + t_0\tilde{t}_1 + t_0 t_1\tilde{t}_2 + \cdots + t_0 t_1 t_2\cdots\tilde{t}_n, \tag{4}$$

where t_n and $\tilde{t}_n$ are obtained

$$t_{n+1} = (1 - t_n\tilde{t}_n - \tilde{t}_n t_n)^{-1} t_n^2$$

and

$$\tilde{t}_{n+1} = (1 - t_n\tilde{t}_n - \tilde{t}_n t_n)^{-1}\tilde{t}_n^2, \tag{5}$$

iteratively. In the calculation the initial condition $t_0=(\epsilon-h_{00})^{-1}h_{10}$ and $\tilde{t}_0=(\epsilon-h_{00})^{-1}h_{01}$ are iterated. The procedure is stopped until the element of the matrix t_n and $\tilde{t}_n$ are small enough to be neglected.

In the investigation of the shot noise, the Fano factor γ over a frequency range $\Delta\nu$ will be calculated. The Fano factor is a measure of the deviation from the classical Poissonian behavior and is expressed in the form of

$$\gamma = \frac{\langle(\Delta I)^2\rangle}{(2e/h)\Delta\nu I}, \tag{6}$$

where $\langle(\Delta I)^2\rangle$ is the current fluctuation and is found to be[29]

$$\langle(\Delta I)^2\rangle = \frac{2e^2\Delta\nu}{h}\,\mathrm{Tr}[(1-T)T]|eV| \tag{7}$$

at the small bias V and low temperature limit. For a perfect CNT, the electrons transmit through the CNT without reflection; the shot noise is, therefore, fully suppressed which can be reached directly from the Landauer-Büttiker formula.

III. RESULTS AND DISCUSSION

A. Numerical results of conductance and shot noise

The conductance and the shot noise of CNTs with two defects at different spatial locations have been calculated numerically. We will focus on the effect of the relative distance of defects on the transport properties. In the calculation of the electronic structure of SWNT's, a tight-binding model is adopted in which one π electron orbital per carbon atom is kept and the on-site energy is taken to be zero. The constant nearest-neighbor carbon bond hopping integral γ_0 is chosen as -3.0 eV.

Because two carbon atoms A and B in an unit cell of graphite belong to two different sublattices, the defect can occupy one of the lattice sites. Therefore, the configurations of CNT with two pointlike defects can be classified into two different types: AA type and AB type. For the AA-type configuration, the two defects locate at the same sublattice, i.e., $\lambda=0$; while for the AB type, one defect locates at the A sublattice and another one locates at the B sublattice, i.e.,

$\lambda=1$. The most interesting property in the charge transport is mainly characterized by those electronic properties near the Fermi energy. We will first discuss this energy region in detail. For a metallic CNT, the Fermi "surface" is described by two points $\mathbf{K}$ and $\mathbf{K}'$ which satisfy $\mathbf{K}-\mathbf{K}'=(\frac{1}{3})(\mathbf{b}_1-\mathbf{b}_2)$, where $\mathbf{b}_1$ and $\mathbf{b}_2$ are reciprocal lattice vectors as shown in Fig. 1. Under the Born approximation, the matrix element near the Fermi points of two pointlike potentials can be written in the form of

$$\langle \mathbf{K}|V(\mathbf{r})|\mathbf{K}'\rangle = \langle \mathbf{K}|g\,\delta(\mathbf{r})|\mathbf{K}'\rangle + \langle \mathbf{K}|g\,\delta(\mathbf{r}-\mathbf{\Delta}d)|\mathbf{K}'\rangle = (1+\phi)\langle \mathbf{K}|g\,\delta(\mathbf{r})|\mathbf{K}'\rangle, \quad (8)$$

where $\phi=\exp[-i(\mathbf{K}-\mathbf{K}')\cdot\Delta\mathbf{d}]$. From Eq. (1) it is found $\phi=\exp[-i(2\pi/3)(l_1-l_2)]$.

First, we discuss the *AA*-type configuration of paired defects. In the evaluation of the matrix element $\langle \mathbf{K}|V(\mathbf{r})|\mathbf{K}'\rangle$, it is found that there are only three different possible values, which correspond to three different kinds of configurations of paired defects respectively, i.e., $l_1-l_2=3N+1$, $3N+2$, and $3N$. For these three configurations, the corresponding values of ϕ are $\phi=\omega$, $\phi=\omega^2$, and $\phi=1$, respectively, where $\omega\equiv\exp[i(2\pi/3)]$. It is noted that the configurations of $l_1-l_2=3N+1$, and $l_1-l_2=3N+2$ or $3N-1$ are equivalent because their matrix elements are mutually conjugated. Based on these analyses we can conclude that there are only two typical behaviors for conductances in the region near the Fermi energy at $\epsilon_F=0$. It should be pointed out that for any metallic CNTs, such a classification is independent of the choice of $\Delta\mathbf{d}$. In general, $\Delta\mathbf{d}$ is not unique due to the cylindrical structure of CNTs so that we can define a different $\Delta\mathbf{d}'$ which satisfies $\Delta\mathbf{d}'=\mathbf{C}-\Delta\mathbf{d}$, where $\mathbf{C}=n\mathbf{a}_1+m\mathbf{a}_2$ is the circumference of metallic CNT. Because of its metallic character, we have the relation $n-m=3K$. Hence, $\Delta\mathbf{d}'$ and $\Delta\mathbf{d}$ belong to the same class.

For different configurations of paired defects in a (6,6) nanotube, the conductance and the Fano factor as the functions of Fermi energy are shown in Fig. 2 ($n_d-m_d=3N$) and Fig. 3 ($n_d-m_d=3N\pm1$), respectively. It is found that the behaviors for the configurations $n_d-m_d=3N$ and $n_d-m_d=3N\pm1$ are completely different in the region near the Fermi energy $\epsilon_F=0$. The conductance is reduced by one unit $G_0=2e^2/h$ for $n_d-m_d=3N$ while is dropped to zero for $n_d-m_d=3N\pm1$. From our previous qualitative analysis, the prefactor of $\langle \mathbf{K}|V(\mathbf{r})|\mathbf{K}'\rangle$ [see Eq. (8)] for the case of $n_d-m_d=3N$ is real and has the maximum value. This leads to the finite value of transmission when the Fermi energy is set to be zero. If $n_d-m_d=3N\pm1$ this prefactor is complex and results in significant destructive interference. Furthermore, it is shown that the shot noise is fully suppressed for the configuration $n_d-m_d=3N$ (Fig. 2). This indicates that only one eigenchannel is open if paired defects satisfy $n_d-m_d=3N$. However, for the case of $n_d-m_d=3N\pm1$, all eigenchannels have been closed at the regime near the zero Fermi energy, so the shot noise reaches its maximum value. By increasing the Fermi energy, the second channel is opened so that the transmission is enhanced and the conductances jump to $2G_0$ near the energy of $\epsilon=1.470$ eV in both cases of Figs. 2 and 3, abruptly. This difference in the conductance for two different defect configurations will be further discussed in the next section using the effective mass theory.

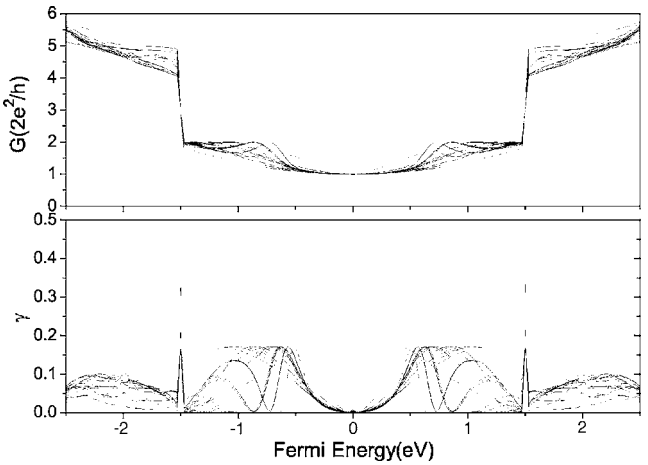

FIG. 2. The conductance (upper panel) and the Fano factor (lower) vs energy for (6,6) CNTs in the presence of two defects, which are in same sublattice. The relative distance $\Delta\mathbf{d}=n_d\mathbf{a}_1+m_d\mathbf{a}_2$ satisfying $n_d-m_d=3N$ or $\phi=1$. The distance $\Delta\mathbf{d}$ is much greater than the C-C bond length.

For the *AB*-type configurations of paired defects on CNT, these two defects are located at two different sublattices. Thus, we have $\lambda=1$ and $\Delta\mathbf{d}=l_1\mathbf{a}_1+l_2\mathbf{a}_2+\mathbf{t}$. Similar to the *AA*-type configuration, the corresponding classification can also be defined in terms of the phase factor ϕ. The ϕs can still take three different values only: ω, ω^2, and 1. For the case of $\phi=1$, the conductance and the Fano factor are plotted in Fig. 4. It is found that near to $\epsilon_F=0$, the behaviors of the conductance and the Fano factor in the *AB*-type configurations of defects has manifested a similar behavior as those in an *AA*-type configuration of defects with $\phi=\omega$ and ω^2. The conductance is suppressed to zero approximately and the Fano factor reaches to unit, i.e., $\gamma\simeq1$. Figure 5 shows the conductance and the shot noise with ϕ equal to ω or ω^2. It is shown that near $\epsilon_F=0$, the conductance is around G_0 but the

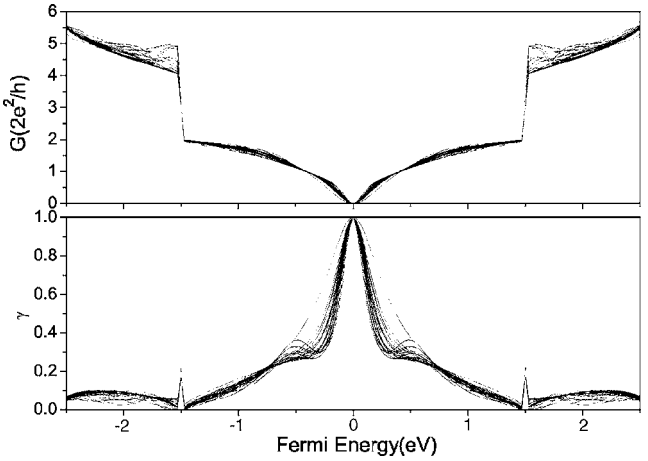

FIG. 3. The conductance (upper panel) and the Fano factor (lower) vs energy for (6,6) CNTs in the presence of two defects, which are in same sublattice. Here $n_d-m_d=3N\pm1$ and $\phi=\omega$ or ω^2. The distance $\Delta\mathbf{d}$ is much greater than the C-C bond length.

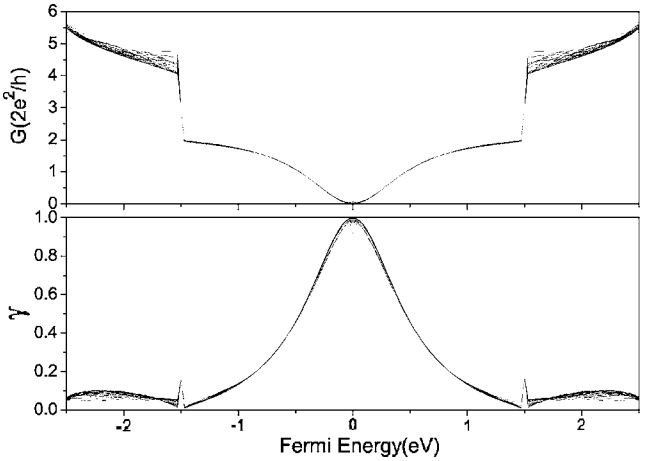

FIG. 4. The conductance and shot noise of a (6,6) SWNT with two defects in different sublattices having $\phi=1$. The distance $\Delta\mathbf{d}$ is much greater than the C-C bond length.

shot noise is dropped to zero which indicates it is suppressed if the distance of two defects is much greater than the length of the C-C bond. For the case of these two defects to be nearest neighbors, the conductance at $\epsilon_F=0$ is a little smaller than $2G_0$.[30] It is worth emphasizing that although the above results are obtained for (6,6) nanotubes, they are generally applicable to metallic tubes and do not depend on the chirality of the CNTs. Such a classification for the transport properties in metallic CNTs can be regarded to be universal.

In order to see the variance of the conductance and the Fano factor with the separations of two defects in *AB*-type configuration, the conductance and the Fano factor have been investigated with the different $\Delta\mathbf{d}$. Figure 6 shows that for $\phi=1$ while Fig. 7 for $\phi=\omega$ or ω^2. It is shown that if the distance $\Delta\mathbf{d}$ is much larger than the C-C bond length (more than $10a_c$), the electron band structure would not be changed by the variance of a relative distance between these two individual defects significantly and the conductance and the shot noise of tubes depend on the phase factor ϕs. This indicates that these two defects act as two isolated scattering

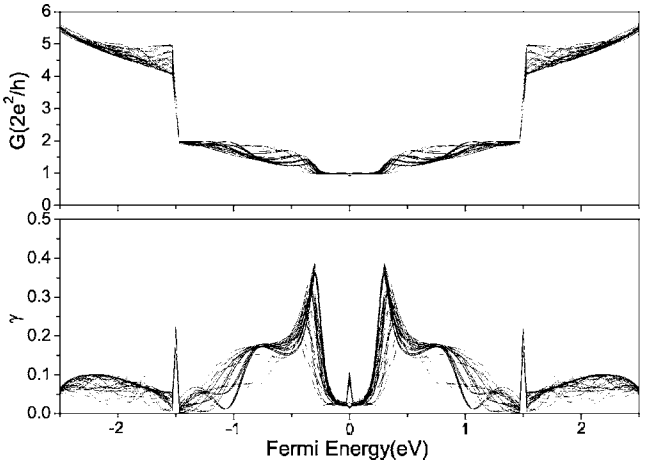

FIG. 5. The conductance and shot noise of a (6,6) SWNT with two defects in different sublattices having $\phi=\omega$ or ω^2. The distance $\Delta\mathbf{d}$ is much greater than the C-C bond length.

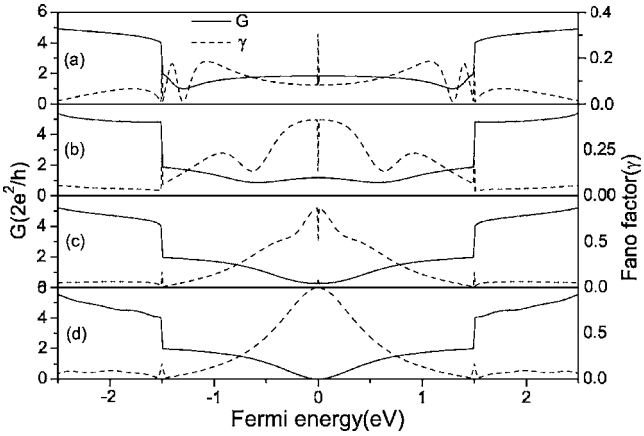

FIG. 6. The conductance (solid line) and Fano factor (dashed line) vs Fermi energy for the (6,6) SWNT with two defects in different sublattices having $\phi=1$. The relative distance of the two defects are (a) $|\Delta\mathbf{d}|=a_c$, (b) $5a_c$, (c) $8a_c$, and (d) $\sqrt{259}a_c$.

centers. As shown in the two lower panels in Figs. 6 and 7, the interference of electrons scattered off the two separated scattering centers results in an oscillatory behavior in the conductance and the shot noise. The behaviors near $\epsilon_F=0$ are dramatically related to the relative distance of two defects.

In comparison to that of large separation of two defects, properties of the transport are quite different when $\Delta\mathbf{d}$ is comparable to the C-C bond length. When the two defects are very close to each other, the electron band structure is significantly altered. It is found that the two upper curves in Fig. 6 are quite similar to that in Fig. 7 so that the dependence of both the conductance and the shot noise on the values of ϕ is not distinct. The reason is that a gap can be generated when the value of $\Delta\mathbf{d}$ is around a_c for any value of ϕ. The gap would disappear when $\Delta\mathbf{d}$ increases slightly.

B. In comparison of the analytic result

To understand the behaviors of the conductance and the shot noise near neutral Fermi energy, we present an analysis

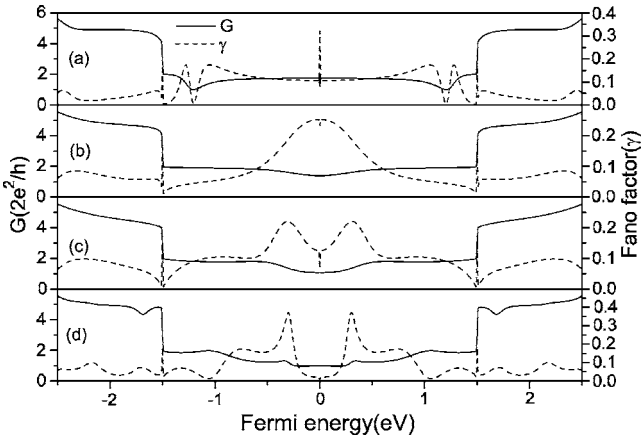

FIG. 7. The conductance (solid line) and Fano factor (dashed line) vs Fermi energy for the (6,6) SWNT with two defects in different sublattices having $\phi=\omega$ or ω^2. The relative distance of the two defects are (a) a_c, (b) $\sqrt{28}a_c$, (c) $\sqrt{109}a_c$, and (d) $\sqrt{373}a_c$.

based on the effective mass theory.[25] To this end, we expand the Hamiltonian at the $\mathbf{K}$ and $\mathbf{K}'$ point and retain the linear terms only. The matrix representation of the potential due to a defect localized at in $\mathbf{r}_0$ is given as,

$$V_A(\mathbf{r}) = g\begin{pmatrix} K_A & K_A' & K_B & K_B' \\ 1 & \alpha & 0 & 0 \\ \alpha^* & 1 & 0 & 0 \\ 0 & 0 & 0 & 0 \\ 0 & 0 & 0 & 0 \end{pmatrix}\delta(\mathbf{r}-\mathbf{r}_0)$$

and

$$V_B(\mathbf{r}) = g\begin{pmatrix} 0 & 0 & 0 & 0 \\ 0 & 0 & 0 & 0 \\ 0 & 0 & 1 & \alpha \\ 0 & 0 & \alpha^* & 1 \end{pmatrix}\delta(\mathbf{r}-\mathbf{r}_0),$$

where $\alpha=\exp[-i(\mathbf{K}-\mathbf{K}')\cdot\mathbf{r}_0]$ and g is the potential strength. There are two right-going channels $\mathbf{K}_+$ and $\mathbf{K}_+'$ as well as two left going channels $\mathbf{K}_-$ and $\mathbf{K}_-'$ in the vicinity of $\epsilon_F=0$. The scattering matrix can be written as

$$S = \begin{array}{c} \\ \mathbf{K}_- \\ \mathbf{K}_-' \\ \mathbf{K}_+ \\ \mathbf{K}_+' \end{array}\begin{array}{c} \begin{array}{cccc} \mathbf{K}_+ & \mathbf{K}_+' & \mathbf{K}_- & \mathbf{K}_-' \end{array} \\ \begin{pmatrix} r_{KK} & r_{KK'} & t'_{KK} & t'_{KK'} \\ r_{K'K} & r_{K'K'} & t'_{K'K} & t'_{K'K'} \\ t_{KK} & t_{KK'} & r'_{KK} & r'_{KK'} \\ t_{K'K} & t_{K'K'} & r'_{K'K} & r'_{K'K'} \end{pmatrix} \end{array}. \tag{9}$$

These analytical results can be applied to the systems for both *AA*-type and *AB*-type configurations.

For the *AA*-type configuration with $n_d-m_d=3N$ and a larger $\Delta\mathbf{d}$, the transmission matrix t can further be written as[25]

$$t = \begin{array}{c} \\ \mathbf{K}_+ \\ \mathbf{K}_+' \end{array}\begin{array}{c} \begin{array}{cc} \mathbf{K}_+ & \mathbf{K}_+' \end{array} \\ \begin{pmatrix} \frac{1}{2} & -\frac{1}{2}e^{-i(\mathbf{K}-\mathbf{K}')\cdot\Delta\mathbf{d}} \\ -\frac{1}{2}e^{i(\mathbf{K}-\mathbf{K}')\cdot\Delta\mathbf{d}} & \frac{1}{2} \end{pmatrix} \end{array}. \tag{10}$$

By using the formulas of conductance and the shot noise it is obtained $G=G_0$ and $\gamma=0$. Therefore, the shot noise is fully suppressed at $\epsilon_F=0$. Since the two defects at the equivalent sites produce quasibound states of the same energy level, it is equivalent to the situation of a single defect on the tube with strength $2g$. Therefore the results given here are very similar to those for a single defect.[12,31] The above analysis is in agreement with the numerical result in Fig. 2.

However, for an *AA*-type configuration with $n_d-m_d=3N\pm1$ and larger $\Delta\mathbf{d}$, the transmission matrix can be written as

$$t = \begin{pmatrix} 1-\dfrac{ig}{\gamma_0 L+igg_0} & 0 \\ 0 & 1-\dfrac{ig}{\gamma_0 L+igg_0} \end{pmatrix}, \tag{11}$$

where L is the circumference of CNT and g_0 is found to be[25]

$$g_0(x,y) = \frac{-i}{\pi\gamma_0}\int du_y \sum_n \frac{\epsilon e^{iu_x(n)x+iu_y y}}{[u_x(n)^2+u_y^2]-(\varepsilon/\gamma_0+i0)^2}$$

with $u_x(n)=(2\pi n/L)-K_x$ and $u_y=k_y-K_y$. Here $\epsilon=|\gamma_0|\sqrt{u_x(n)^2+u_y^2}$.

Then, it is obtained the analytical expressions for the conductance

$$G = 2\frac{2e^2}{h}\frac{\gamma_0^2L^2+g^2(g_0-1)^2}{\gamma_0^2L^2+g^2g_0^2}$$

and the shot noise

$$S_I = 4\frac{e^2}{h}|eV|2\frac{[\gamma_0^2L^2+g^2(g_0-1)^2](2g_0-1)g^2}{(\gamma_0^2L^2+g^2g_0^2)^2}.$$

Near the Fermi energy $\epsilon_F=0$, we have $g_0\simeq1$. In the limit of the larger potential strength $g\to\infty$, we have $G\approx0$ and $\gamma\approx1$. This is in agreement with the numerical result in Fig. 3.

For an *AB*-type configuration, the conductance behavior is reversed to those in *AA*-type configurations as seen in Figs. 4 and 5 if the distance of two pointlike potentials is far enough (more than 20 nm). The conductance at $\epsilon_F=0$ equals G_0 for $\phi=\omega$ or ω^2 and is dropped to zero for $\phi=1$. However, there is no simple analytical solution for this. It has been shown that the relative distance of two defects will change the levels of quasibound states.[30] If these two defects are closer to each other, the quasibound states would be generated. Such quasibound states are similar to the "bonding" and "antibonding" states which can be constructed from two inequivalent states ψ_A and ψ_B.[30] The separation between bonding and antibonding states would be decreased with increasing $\Delta\mathbf{d}$. If the relative distance is larger than that of C-C bond, the separation tends to zero and results in a minimum value in the conductance, as shown in Figs. 6(d) and 7(d).

IV. SUMMARY AND CONCLUSIONS

In summary, we have studied the electron transport in metallic CNTs with two localized scattering centers within the π-electron tight-binding model. The oscillations in the conductance and the Fano factor caused by the interference of waves scattered from the different defects have been shown. It is found that the conductance and the shot noise are strongly dependent on the phase factor ϕ which is generated by the scattering. For *AA*-type configurations of defects (i.e., two defects are in the same sublattice) and $\Delta\mathbf{d}\gg a_c$, the conductance near the neutral Fermi energy is dropped to G_0 and the shot noise decreases to zero when $\phi=1$ but it decreases to zero and the Fano factor reaches the unit if $\phi=\omega$ or ω^2, whereas, the situation is reversed for *AB*-type configurations of defects. If $\Delta\mathbf{d}$ is around a few a_c, a small "gap" would be developed at $\epsilon_F=0$. This rule is applicable to all metallic CNTs and is independent of the chirality of CNTs.

ACKNOWLEDGMENTS

Authors would like to thank Jian Wang and Wei Ren for valuable discussions. This work was supported by NNSFC Grant No. 10474002 and by the Australian Research Council.

[1] S. Iijima, Nature (London) **354**, 56 (1991).
[2] N. Hamada, S. I. Sawada, and A. Oshiyama, Phys. Rev. Lett. **68**, 1579 (1992).
[3] J. W. Mintmire, B. I. Dunlap, and C. T. White, Phys. Rev. Lett. **68**, 631 (1992).
[4] R. Saito, M. Fujita, G. Dresselhaus, and M. S. Dresselhaus, Appl. Phys. Lett. **60**, 2204 (1992).
[5] R. Saito, M. Fujita, G. Dresselhaus, and M. S. Dresselhaus, Phys. Rev. B **46**, 1804 (1992).
[6] M. S. Dresselhaus, G. Dresselhaus, and R. Saito, Phys. Rev. B **45**, 6234 (1992).
[7] R. A. Jishi, M. S. Dresselhaus, and G. Dresselhaus, Phys. Rev. B **47**, 16671 (1993).
[8] S. V. Rotkin and K. Hess, Appl. Phys. Lett. **84**, 3139 (2004).
[9] R. Saito, M. S. Dresselhaus, and G. Dresselhaus, *Physical Properties of Carbon Nanotubes* (Imperial College Press, London, 1998).
[10] M. Ouyang, J. L. Huang, C. L. Cheung, and C. M. Lieber, Science **292**, 702 (2001).
[11] A. V. Krasheninnikov, K. Nordlund, and J. Keinonen, Phys. Rev. B **65**, 165423 (2002).
[12] L. Chico, L. X. Benedict, S. G. Louie, and M. L. Cohen, Phys. Rev. B **54**, 2600 (1996); H. J. Choi, J. Ihm, S. G. Louie, and M. L. Cohen, Phys. Rev. Lett. **84**, 2917 (2000).
[13] M. Igami, T. Nakanishi, and T. Ando, J. Phys. Soc. Jpn. **68**, 716 (1999).
[14] J. Park, Y. Yaish, M. Brink, S. Rosenblatt, and P. L. McEuen, Appl. Phys. Lett. **80**, 4446 (2002).
[15] A. Rubio, S. P. Apell, L. C. Venema, and C. Dekker, Eur. Phys. J. B **17**, 301 (2000).
[16] T. D. Yuzvinsky, A. M. Fennimore, W. Mickelson, C. Esquivias, and A. Zetti, Appl. Phys. Lett. **86**, 053109 (2005).
[17] M. Büttiker, J. Math. Phys. **37**, 4793 (1996).
[18] G. Iannaccone, G. Lombardi, M. Macucci, and B. Pellegrini, Phys. Rev. Lett. **80**, 1054 (1998).
[19] O. M. Bulashenko, J. M. Rubí, and V. A. Kochelap, Phys. Rev. B **61**, 5511 (2000).
[20] M. Büttiker, Phys. Rev. Lett. **65**, 2901 (1990).
[21] Y. Wei, B. Wang, J. Wang, and H. Guo, Phys. Rev. B **60**, 16900 (1999).
[22] Y. M. Blanter and M. Büttiker, Phys. Rep. **336**, 1 (2000).
[23] P. E. Roche, M. Kociak, A. Kasumov, B. Reulet, and H. Bouchiat, Eur. Phys. J. B **28**, 217 (2002).
[24] N. Y. Kim, W. D. Oliver, Y. Yamamoto, J. Kong, and H. Dai, cond-mat/0311434.
[25] T. Ando, T. Nakanishi, and M. Igami, J. Phys. Soc. Jpn. **68**, 3994 (1999).
[26] S. Datta, *Electronic Transport in Mesoscopic System* (Cambridge University Press, Cambridge, 1995).
[27] M. P. Lopez Sancho, J. M. Lopez Sancho, and J. Rubio, J. Phys. F: Met. Phys. **14**, 1205 (1984).
[28] M. P. Lopez Sancho, J. M. Lopez Sancho, J. M. L. Sancho, and J. Rubio, J. Phys. F: Met. Phys. **15**, 851 (1985).
[29] D. Orlikowski, H. Mehrez, J. Taylor, H. Guo, J. Wang, and C. Roland, Phys. Rev. B **63**, 155412 (2001).
[30] H. F. Song, J. L. Zhu, and J. J. Xiong, Phys. Rev. B **65**, 085408 (2002).
[31] T. Kostyrko, M. Bartkowiak, and G. D. Mahan, Phys. Rev. B **60**, 10735 (1999).